

Study on Model Simulation Design Based on Open CASCADE Platform

Mingxia Zhao

State Grid Jibei Electric Power Company Limited Skills Training Center

Baoding Electric Power VOC. & TECH.

College, Baoding

Hebei, China

E-mail: 879527755@qq.com

Abstract—CAD-based geometric design has been widely used in various industries in the society. With the continuous improvement of design complexity, higher requirements are placed on the model simulation design of high-precision and high-confidence. The paper analyzes the simulation process of 3D model and improves the feature extraction method in the process based on the research of OpenCASCADE platform. Firstly, the CAD platform geometry model is used to develop the model concept map, and then the model's three-view projection map is used to extract feature information; meanwhile, the complex surface adjustment and description are used to represent the model feature information. Finally, the graph feature vector obtained by the complex facet and transformation is calculated by using the maximum and minimum approximations as the distance between the feature references, so as to evaluate the similarity between the models. the experiment have shown that the projection mapping of complex surface adjustment can accurately identify the fluctuations of complex surfaces in the model, and facilitate the more precise acquisition of feature parameters. The related functions studied in the paper will help to further improve the development capability of 3D models based on OpenCASCADE, which can make the faster implementation of high-precision simulation design requirements.

Keywords-OpenCASCADE; CAD; Model Simulation

I. INTRODUCTION

Model processing and expression in the mechanical design drawing is inseparable from CAD model. The effect display of CAD model can be used to perform

three-dimensional rotation and perspective special effects inspection to represent the completeness of model establishment. However, it is much more complicated to copy the prototype only in the case of a prototype. First, since the precise parameters of the original object are not grasped that require a series of measurement and conceptualization processes, but the details of the measurement and expression of the original object are not accurate enough, the deviation of the retrieval precision is easily generated, which requires and calculates the physical object to be prototyped and a more adequate description, so as to obtain accurate model parameters[1-3].

II. MODEL SIMULATION PROCESS AND ALGORITHM PRINCIPLE

A. Model simulation process

The model simulation design in the paper is taken as the research object, and a representation method for complex surface adjustment and reconciliation is proposed. The box screening of the surface adjustment of the original physical model is carried out, and the model projections of different complexity levels are applied to different packaging boxes for feature vector extraction[4]. Firstly, the user applies the CAD model projected in the model library to extract the feature information according to the conceptual design requirements and extracts the feature information, and uses the complex facet and descriptor to represent the feature information. Finally, the target model is returned from the database according to the feature information similarity measure result, and pushed to the users; the implementation process is shown in Figure 1.

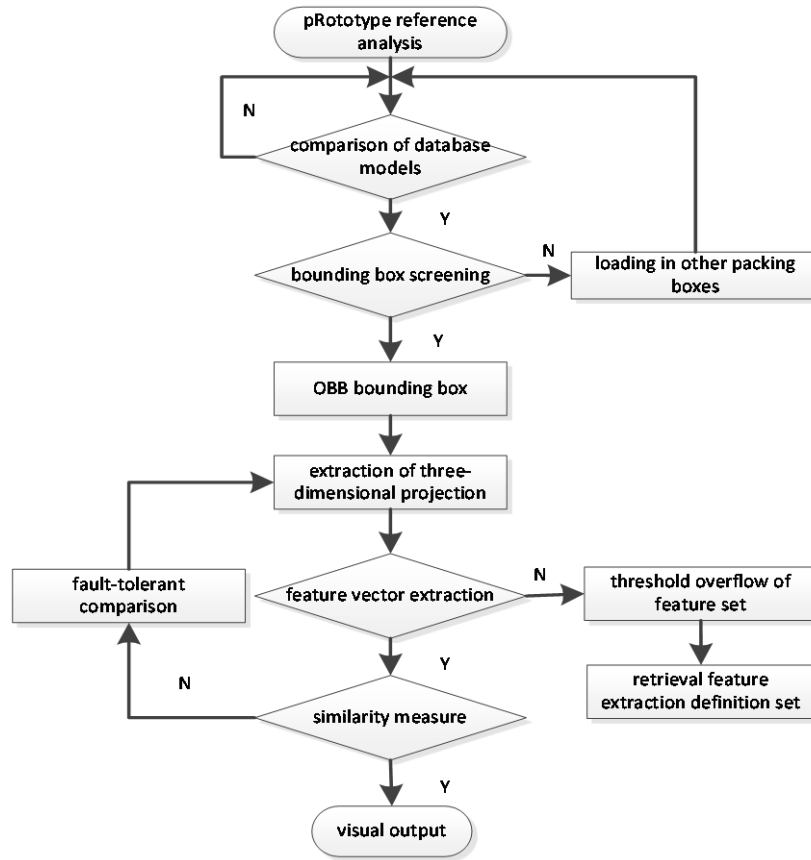


Figure 1. Process of model simulation design

B. Model geometry metric

In order to accurately identify and screen small, narrow and irregular objects in large-scale complex CAD models, a method in the paper is proposed to measure the size and space occupancy of the model.

1) Model size metric based on approximate minimum bounding box

Due to the advantages of simple calculations and small storage space, AABB bounding boxes and bounding spheres in computer graphics are widely used for approximating expressions of primitive geometric models for such things as collision/intersection calculations, occlusion queries, etc. However, the encircled ball contains too much redundant volume; while the faces of the AABB bounding box are axially parallel, it is easy to be affected by the direction of the model that have with uneven distribution in three axial directions, which is as shown in Figure 2. Therefore, the accuracy of the approximate calculation of the model size of

using the volume of the OBB bounding box is more accurate .

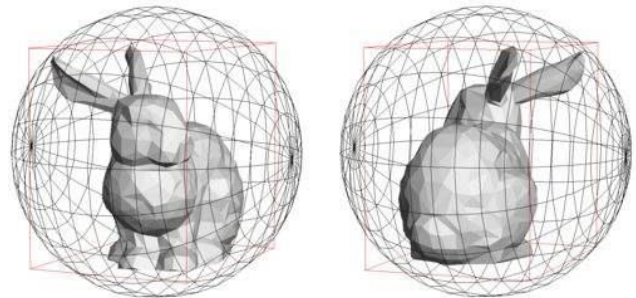


Figure 2. Extracting model features using OBB bounding box

Based on the above analysis, the approximate minimum bounding box (or Oriented-Bounding-Box, OBB) volume in the paper is used as an approximate calculation of the model size. Approximate minimum bounding box is calculated using a method based on covariance matrix.

C. Algorithm principle

In mathematical statistics, for two-dimensional random variables (X, Y), in addition to the mean, standard deviation, and variance, the covariance is described as a linear correlation between X and Y. The equation of calculating the covariance $cov(X, Y)$ is as follows.

$$cov(x, y) = E\{[x - E(x)][y - E(y)]\} \quad (1)$$

Where, E represents the expected value of the variable. The smaller the covariance, the more independent the two variables are, namely, the linear correlation is small.

A three-dimensional random variable (x, y, z) is constructed by inputting the vertex coordinates (x_i, y_i, z_i) of the model. The above covariance calculation formula is used to establish a covariance matrix, which is as follows.

$$a = \begin{cases} cov(x, x) & cov(x, y) & cov(x, z) \\ cov(x, y) & cov(y, y) & cov(y, z) \\ cov(x, z) & cov(y, z) & cov(z, z) \end{cases} \quad (2)$$

Where, the leading diagonal element is actually the variance of the variable, and the non-diagonal element represents the covariance between the variables. The elements of the covariance matrix are real and symmetric. The covariance matrix defines the propagation (variance) and direction (covariance) of the vertex data. The similar transformation of the covariance matrix is as follows.

$$a = \begin{bmatrix} \alpha_1 & \alpha_4 & \alpha_7 \\ \alpha_2 & \alpha_5 & \alpha_8 \\ \alpha_3 & \alpha_6 & \alpha_9 \end{bmatrix} \begin{bmatrix} \chi^1 \\ \chi^2 \\ \chi^3 \end{bmatrix} \begin{bmatrix} \beta_1 & \beta_4 & \beta_7 \\ \beta_2 & \beta_5 & \beta_8 \\ \beta_3 & \beta_6 & \beta_9 \end{bmatrix} \quad (3)$$

The last three matrices in the equation are that the last one is the inverse matrix of the first one, and the middle one is the diagonal matrix; then the three eigenvectors of A are $v_1 = (a_1, a_2, a_3)^K$, $v_2 = (a_4, a_5, a_6)^K$, $v_3 = (a_7, a_8, a_9)^K$, respectively; these three feature vectors are approximate the

direction of the 3 axes of the minimum bounding box; wherein the feature vector corresponding to the largest feature value points to the direction of the maximum variance of the data, which is the longest axis direction of the model, and each vertex is separately projected on three axes to easily obtain the center point of the approximate bounding box and the length and width of the bounding box. Using the above method to obtain an approximate minimum bounding box result, the approximate minimum bounding box is more compact than other bounding boxes, and its size is not affected by the geometric model rotating in three dimensions. Therefore, it is more accurate to describe the size of the geometric model with the volume of the approximate minimum bounding box[5]. As a result, the OBB bounding box is taken as the best solution in the approximate minimum bounding box of the complex shape object of the model. The process is mainly to calculate the volume of each object and approximate the bounding box and sort it, so that different sizes of objects can be selected in the model.

III. OPTIMIZATION PROCESSING OF COMPLEX SURFACE FEATURE VECTOR EXTRACTION

A. Three-dimensional space function representation

It needs to be spatially processed by the model after the OBB bounding box determines the model features. The detailed steps for converting the 2D graphics acquired by the projection into 3D space are as follows.

Step1. For a model part, the acquired complex surface projection image forms a 2D image, and a bounding sphere is constructed. The center of the surrounding sphere is located at the origin of the coordinate system xyz, which satisfies three conditions: 1) the center of the encircled ball corresponds to the center of the smallest bounding box of model A; 2) the radius of the surrounding sphere is 1/2 of the diagonal length of the minimum bounding box of model A; 3) The model A is located on the equatorial plane surrounding the ball S, which is located on the coordinate plane xy of the coordinate system xyz.

Step2. A series of rays are generated from the center of the surrounding sphere, and the intersection of these rays

with the model A is calculated, so that the model A can be approximated representation by these intersection points, which is the $A = \{p_i\}$, and is as shown in Fig 3. Assuming that the angle between a certain ray r_i and the coordinate axis x is θ_i , and the distance between the intersection p_i of the ray r_i and the model A and the center of the surrounding sphere is d_i , the intersection p_i can be expressed as $p_i = f(\theta_i, d_i)$ in the two-dimensional space. Another variable QQ is introduced for converting the engineering model A into a

three-dimensional space, which is defined as: $\phi_i = \arctan(d_i / r)$, where r is the radius surrounding the sphere. Therefore, the transformation intersection point p_i in the form of a complex surface function $p_i = f(\theta_i, \phi_i, d_i)$, in which case each intersection point p_i has a unique (θ_i, ϕ_i) corresponding to it in the three-dimensional space. As a result, the model A has a one-to-one correspondence with complex surface functions.

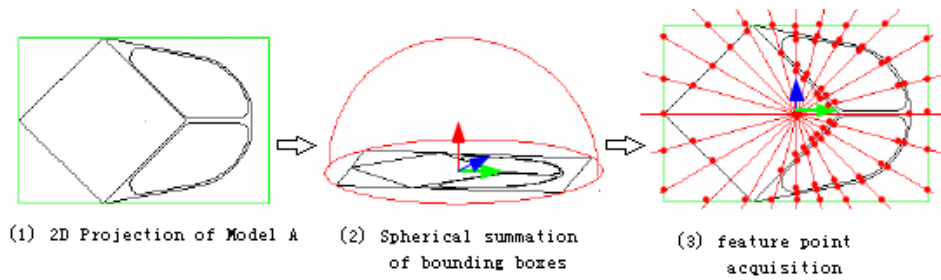


Figure 3. ComplexSurfaceRepresentationofModelA

B. Feature Vector Extraction of Model Complex Surfaces

In order to obtain the rotation invariant of the model projection surface, 2B Chebyshev data points are sampled on the complex surface function with bandwidth B using the fast complex surface and transformation method. The complex surface and descriptor extraction steps of model A are as follows.

Step1. Data point sampling on model A.

2B rays are extracted from the center of the minimum bounding box of the model A, and the intersection of the ray and the model A is: $p_i = f(\theta_i, d_i)$, and the position of the sampling point in the three-dimensional space is calculated according to the equation(1).

$$\begin{cases} \theta_i = (i + 0.5) \frac{\pi}{B} \\ \phi_i = \arctan \frac{d_i}{r} \end{cases} \quad (i = 0, 1, 2, \dots, 2b - 1) \quad (4)$$

Step1. The Chebyshev point position of the sampling point (θ_i, ϕ_i) is calculated.

$$\begin{cases} i = i \\ j = \frac{2b\phi_i}{\pi} - 0.5 \end{cases} \quad (i, j = 0, 1, 2, \dots, 2b - 1) \quad (5)$$

Then model A can be represented by the Chebyshev point position (i, j) , which is

$$d = \{d_i = f(i, j) | i, j = 0, 1, 2, \dots, 2b - 1\} \quad (6)$$

Step2. Normalization.

In general, different graphics have different sizes. If two shapes are the same and the sizes are different that the $\{d_i\}$ is different. Therefore, the graphics need to be normalized. Unification of model A is generally normalized to the long or short side of the minimum bounding box of its model A. The normalization factor of the paper is the radius r of the

bounding sphere, and its normalization is as shown in equation 7.

$$\begin{cases} s = \frac{v}{r} \\ d = \{di \times s = f(i, j) | i, j = 0, 1, 2, \dots, 2b-1\} \end{cases} \quad (7)$$

Where, v is a predefined constant.

Step 4. Fasting and complex surface adjustment and transformation.

The rotation invariant descriptor of model A is obtained by using the method proposed in [16] to perform fast complex surface adjustment and transformation. A corresponding rotation invariant will be obtained for each frequency. The method can avoid the one-to-many correspondence and the instability caused by the shape disturbance, so as to obtain the rotation invariant descriptor of the model A.

Bandwidth B determines the density of the sampling points. When B is small, many details will be lost. When B is large, the model A is more accurate, but the time is relatively large. Therefore, we need to make trade-offs. When the bandwidth B gotten by the experiments is 64, the accuracy is 5×10^{-3} , which can meet the graphics retrieval requirements. As a result, the bandwidth in the paper is set to 64.

C. Feature Vector Similarity Extraction

The similarity comparison problem between the graphics is converted into the distance metric between the feature vectors by using complex surface adjustment and transformation to obtain the feature vectors of the graphics. The Euclidean distance is selected to calculate the distance between the feature vectors. Assuming that the eigenvectors of the two models f and g are $f_{sh} = [|f_o|, |f_1|, \dots, |f_b|]$ and $g_{sh} = [|g_o|, |g_1|, \dots, |g_b|]$, respectively, the similarity distance between the two models is shown in Equation 8.

$$d(f_{sh}, g_{sh}) = \sqrt{\sum_{l=0}^b (|f_l| - |g_l|)^2} \quad (8)$$

IV. MODELING SIMULATION EXPERIMENT

A. Modeling implementation

The OpenCASCADE is modeled based on the BREP method. In the document module generated by the wizard, the parameters of the model are placed in the label of the data frame, and then the modeling function is used to generate the geometric model according to the parameters in the label. We modify the values in the label and reshape them during the modification process. The label framework of the parameter attributes in the data frame can be displayed in the visualization module generated by the wizard. The model can be displayed by associating the model generated in the document module with the corresponding `TPrsStd_AISPresentation` class. The OpenCASCADE modelling is parameter driven and the parameters are saved in the label of the document. Therefore, interactive manipulation of the model can be achieved by modifying the parameters in the label accordingly.

```

Handle(TDocStd_Document)D=GetOCAFDoc();//opena
newdocument
D->NewCommand();
TCollection_AsciiString
Name((Standard_CString)(LPCTSTR)"Sphere");//Namet
hemodel
L_Sphere=TDF_TagSource::NewChild(D->Main());//Cr
eatelabelsunderdocuments
Standard_Realr=50;//Assignmentofmodelparameters
TDataStd_Real::Set(L_Sphere.FindChild(1,r);//Addpara
meterstolabels
TDataStd_Name::Set(L_Sphere,Name);
staticStandard_GUIDanID
("22D22E53-D69A-11d4-8F1A-0060B0EE18E7");
Handle(TFunction_Function)myFunction=
TFunction_Function::Set(L_Sphere,anID);
BRepPrimAPI_MakeSpheremkSphere(r,h);//Establishing
asphericalmodel
ResultShape_Sphere=mkSphere.Shape();
TNaming_BuilderB(L_Sphere);
B.Generated(ResultShape_Sphere);

```

B. Simulation

The complex surface adjustment and extraction descriptions are applied in process of test model simulation design, which can express the quality and effect of model design intuitively and accurately. First, the complex surface adjustment and description sub-hierarchy of model are constructed which is shown in Fig 4. Figures 4a and 4b are two similar graphs, the complex surface of which are similar in shape to the sub-histogram, and the complex surface adjustment and maximum and minimum components of the two figures are also relatively close. The similarity between the graphs of Fig 4a, Fig 4b and Fig 4c is relatively small, and the corresponding complex surface adjustment and the shape of the descriptor histogram are similar to each other. It can be seen from the maximum component of the complex surface adjustment that the maximum component of Figure 4a and Figure 4b is close to 1.5, while the maximum component of Figure 4c is close to 1.1, which proves the accuracy of the research content in practical application.

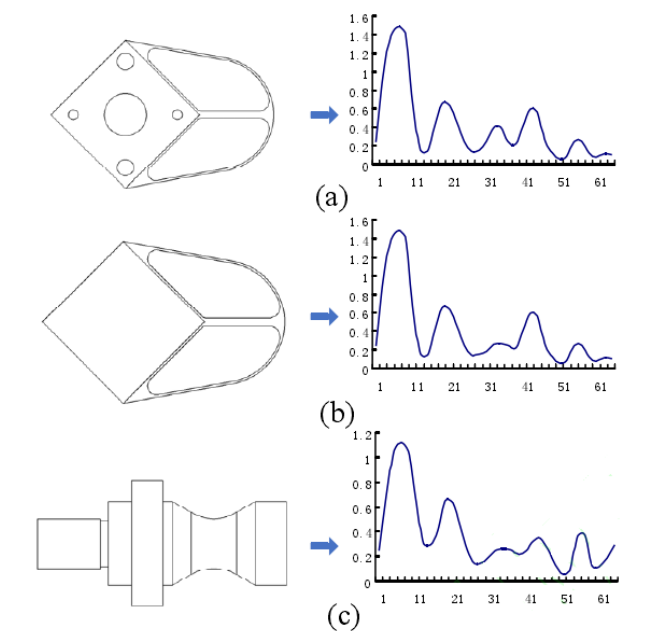


Figure 4. The comparison of complicated surface adjustment and extraction factor component

V. CONCLUSIONS

The development process of the simulation design of the 3D model platform based on OpenCASCADE in the paper is

studied. According to the selection and application of the system mapping box and the optimization of the algorithm, the innovation of extracting the high-precision model imitation design is finally realized. The related functions studied in the paper will help to further improve the development capability of 3D models based on OpenCASCADE, which is bound to have great significance and broad market prospects.

REFERENCES

- [1] E. Zhang, J. Tang, S. Li, P. Wu, J.E. Moses, K.B. Sharpless Chemoselective synthesis of polysubstituted pyridines from heteroaryl fluorosulfates *Chem. Eur. J.*, 22 (2016), pp. 5692-5697.
- [2] Y. Li, G. Wang, G. Hao, J.P. Wang Synthesis of 2,3,5,6-tetrasubstituted pyridines via selective three-component reactions of aldehyde and two different enamines *Tetrahedron Lett.*, 60 (2019), pp. 219-222.
- [3] C. Doebelin, P. Wagner, I. Bertin, F. Simonin, M. Schmitt, F. Bihel, J.J. Bourguignon Trisubstitution of pyridine through sequential and regioselective palladium cross-coupling reactions affording analogues of known GPR54 antagonists *RSC Adv.*, 3 (2013), pp. 10296-10300.
- [4] V.V. Mel'chin, A.V. Butin Furan ring opening–furan ring closure: cascade rearrangement of novel 4-acetoxy-9-furylnaphtho[2,3-*b*]furans *Tetrahedron Lett.*, 47 (2006), pp. 4117-4120.
- [5] C. Balakrishna, V. Kandula, R. Gudipati, S. Yennam, P. Uma Devi, M. Behera An efficient microwave-assisted propylphosphonic anhydride (T3P®)-Mediated one-pot chromone synthesis via enamines *Synlett*, 29 (2018), pp. 1087-1091.